Available online at www.sciencedirect.com
SCIENCE DIRECT®
Acta Materialia 53 (2005) 2169–2179
Acta MATERIALIA
www.actamat-journals.com

Nano-sized twins induce high rate sensitivity of flow stress in pure copper

L. Lu [a,b], R. Schwaiger [c], Z.W. Shan [d], M. Dao [a], K. Lu [b], S. Suresh [a,*]

[a] Department of Materials Science and Engineering, Massachusetts Institute of Technology, Cambridge, MA 02139, USA
[b] Shenyang National Laboratory for Materials Science, Institute of Metal Research, Chinese Academy of Sciences, Shenyang 110016, PR China
[c] Forschungszentrum Karlsruhe, Institute for Materials Research II, 76133 Karlsruhe, Germany
[d] Department of Mechanical Engineering, University of Pittsburgh, Pittsburgh, PA 15261, USA

Received 12 October 2004; received in revised form 21 January 2005; accepted 24 January 2005

Abstract

We have investigated the rate sensitivity of flow stress and the extent of strengthening in polycrystalline copper containing different volume fractions of nano-sized twins, but having the same average grain size. The specimens were produced by pulsed electrodeposition, wherein the concentration of twins was varied systematically by varying the processing parameters. Depth-sensing instrumented indentation experiments performed at loading rates spanning three orders of magnitude on specimens with the higher density of twins (twin lamellae width ~20 nm) revealed an up to sevenfold increase in rate-sensitivity of hardness compared to an essentially twin-free pure Cu of the same grain size. A reduction in twin density for the same grain size (with twin lamellae width ~90 nm) also resulted in a noticeable reduction in rate-sensitivity and hardness. The presence of a high density of nano-scale twins is also seen to impart significant hardness, which is comparable to that achieved in nano-grained Cu. Post-indentation analyses of indented Cu with nano-scale twins in the transmission electron microscope reveal deformation-induced displacement of coherent twin boundaries (CTBs), formation of steps and jogs along CTBs, and blockage of dislocations at CTBs. These processes appear to significantly influence the evolution of thermal activation volume for plastic flow which is some three orders of magnitude smaller than that known for microcrystalline Cu. Transmission electron microscopy also reveals CTBs with a high density of dislocation debris and points to the possibility that displaced CTBs may serve as barriers to dislocation motion and that they may also provide sources for dislocation nucleation, especially near stress concentrations, very much like grain boundaries. Possible consequences of these trends for deformation are explored.

Keywords: Nanostructured metals; Twins; Copper; Nanoindentation; Rate sensitivity; Activation volume

1. Introduction

The strengthening of engineering metals and alloys through grain size reduction has long been a strategy for microstructure design [1,2]. Studies of nanostructured materials in the past two decades have shown that grain refinement in the nanometer range leads to substantial strengthening where abundant grain boundaries (GBs) create obstacles to dislocation motion [3–7].

Recent experimental observations have led to the discovery that nanostructured metals, with average grain size and range of grain size typically smaller than 100 nm, exhibit deformation characteristics that are highly sensitive to the rate of loading [8–11]. Uniaxial tensile experiments in electrodeposited nanocrystalline Cu [8] and tensile [9,10] and depth-sensing indentation [11] experiments in electrodeposited nanocrystalline Ni have established that an increase in loading/strain rate

* Corresponding author. Tel.: +1 617 253 3320; fax: +1 617 253 0868.
E-mail address: ssuresh@mit.edu (S. Suresh).

1359-6454/$30.00
doi:10.1016/j.actamat.2005.01.031

results in a pronounced increase in resistance to plastic flow. A systematic comparison by Schwaiger et al. [11] of loading rate and strain rate under controlled indentation of nominally defect-free, pure, electrodeposited Ni showed that nanocrystalline specimens (average grain size ~40 nm) were highly sensitive to the rate of deformation. However, microcrystalline (average grain size >1 μm) and ultra-fine crystalline (average grain size ~200 nm) specimens exhibited flow behavior that was relatively insensitive to the rate of loading. Strain-rate jump tests [12,13] performed on ultra-fine crystalline copper (average grain size ~200 nm) produced by equal-channel angular pressing (ECAP) with very high initial defect density, on the other hand, showed a strong rate-sensitivity of plastic flow.

The strain rate sensitivity of a ductile metal in uniaxial deformation is commonly written (e.g. see Refs. [12,14]) as

$$m = \frac{\sqrt{3}kT}{v^*\sigma} = \frac{3\sqrt{3}kT}{v^*H}, \tag{1}$$

where m is a non-dimensional rate-sensitivity index, k is the Boltzmann constant, T is the absolute temperature, σ is the flow stress, H is the hardness (which is usually assumed to be three times the flow stress) and v^* is the activation volume which is the rate of decrease of the activation enthalpy with respect to flow stress at a fixed temperature:

$$v^* = \sqrt{3}kT\left(\frac{\partial \ln \dot{\varepsilon}}{\partial \sigma}\right), \tag{2}$$

where $\dot{\varepsilon}$ is the strain rate. The rate-sensitivity parameter m and the activation volume v^* provide quantitative measures of the sensitivity of flow stress to loading rate and also give insights into the deformation mechanisms. Experimental studies suggest that the strain rate sensitivity m of initially (nominally) defect-free nanocrystalline (NC) Cu and Ni is several times higher than that for the microcrystalline (MC) counterpart [8–11]. Furthermore, while the activation volume of conventional microcrystalline face-centered cubic (fcc) metals is on the order of $\sim 1000b^3$, where b is the magnitude of the Burgers vector, the corresponding value for nanocrystalline fcc metals exhibiting enhanced rate sensitivity of plastic flow was found to be reduced by nearly two orders of magnitude (e.g. see Ref. [12]).

Like conventional grain boundaries, coherent twin boundaries (CTBs) can also obstruct the motion of dislocations [15]. This is the case for deformation, annealing, and growth twins, as long as they have interfaces with identical atomic structures [15]. Early studies of α-brass with twin spacing in the micrometer regime showed that twin boundaries (TBs) are equivalent to conventional GBs with respect to such strengthening phenomena as those arising from the Hall–Petch mechanism [16]. (A detailed review of strengthening due to CTBs in microcrystalline materials along with the associated references can be found in Ref. [15].) Exploiting the possibility that TBs could serve as effective barriers to dislocations, recent work has demonstrated that when nano-scale twins are introduced by the pulsed electrodeposition process in polycrystalline Cu and by magnetron sputter deposition in AISI 330 stainless steel [17–19] and in Ni–Co alloys [20], significant strengthening results.

The foregoing considerations naturally lead to two questions which, to our knowledge, have hitherto not been systematically examined:

1. Does the controlled introduction of twins in a polycrystalline fcc metal lead to markedly enhanced rate-sensitivity of plastic flow?
2. If so, what are the mechanistic contributions to such rate-sensitivity of deformation in twinned metals?

Developing an understanding of these issues would provide valuable insights into the mechanical deformation characteristics of a variety of engineering metals and alloys, in which twinning is a prominent mode of deformation. Such an understanding would also offer helpful information for microstructure design of engineering alloys wherein twinning is purposely orchestrated at the processing stage. Furthermore, elevated rate sensitivity may delay necking during tensile deformation and can possibly contribute to ductility. Therefore, fabrication steps that employ such methods as superplastic forming would also benefit from an improved understanding of the connections between twinning and rate-sensitivity of deformation.

In this work, we report a series of systematic experiments that demonstrate that controlled introduction of nano-sized twins in pure copper leads to a significant increase in the rate-sensitivity of plastic flow. For this purpose, we have produced specimens with different volume fractions of nano-sized twins in ultrafine-crystalline (UFC) Cu by recourse to pulsed electrodeposition, while keeping the grain size of the different specimens roughly the same. The rate sensitivity of plastic deformation was studied using depth-sensing instrumented indentation for which the loading rate was varied by three orders of magnitude. Significantly higher loading rate sensitivity is observed for the higher density of twin boundaries. Possible mechanisms contributing to this effect are explored.

2. Materials and experimental methods

2.1. Materials

High purity Cu sheets (20 mm × 10 mm × 0.1 mm in size) with nano-sized growth twin lamellae were synthe-

sized using pulsed electrodeposition from an electrolyte of $CuSO_4$. The procedure is described in detail in [17]. UFC Cu without twins was produced from the same electrolyte using DC electrodeposition.

Chemical analysis of the as-deposited sheet indicated that its purity was better than 99.998 at.%. The densities of all the Cu specimens were measured to be 8.93 ± 0.03 g/cm^3 at room temperature by applying the Archimedes principle.

The foils were polished using SiC paper (grit 4000) and diamond suspensions of 3 and 0.25 μm grain size. The thickness of the twinned Cu layer was estimated to be more than 25 μm after polishing. The UFC Cu foils were polished in the same way and had a final thickness of 500 μm. The specimens were glued onto Al sample holders using standard cyanoacrylate glue.

2.2. Nanoindentation test methods

The hardness was extracted from the indentation data following the procedure outlined in Refs. [21,22]. The unloading curves were shifted to the end of the loading segments in order to compare the hardness at the applied maximum loads and fitted with a power law between 20% and 80% of the maximum load.

A Micromaterials MicroTest 200 indenter (Micromaterials Ltd, Wrexham, UK) equipped with a diamond Berkovich tip was used to test the samples over a wide range of loading rates. Experiments at constant loading rates of 100, 10, 1 and 0.1 mN/s were performed. The loading sequence was as follows. The tip was brought into contact with the material. Subsequently, the specimen was indented at a constant loading rate to a depth of 3 μm. The load was held constant at its maximum value for 10 s. Finally, the samples were unloaded at the respective loading rate to 10% of the maximum load. The load was held constant for 60 s and the displacement data were monitored and used for temperature drift correction. For each sample and loading rate, except the slowest one, at least ten indents were performed. For the slowest loading rate of 0.1 mN/s, five repeat indents were performed. The scatter in the experimental data for all the specimens are indicated along with the trend results.

2.3. Tensile test methods

Tensile tests were performed on a Tytron 250 Microforce Testing System (MTS System Corporation, Eden Prairie, MN, USA) at strain rates in the range of 6×10^{-4} to 6×10^{-1} s^{-1}. A contactless MTS LX300 laser extensometer was used to calibrate and measure the strain of the sample upon loading. The gauge length of dogbone-shaped tensile samples is 4 mm and width is 2 mm, the final thickness after electroposlishing is about 20 μm.

2.4. Microstructure characterization

Microstructures of the specimens in the as-deposited condition as well as after tensile deformation were characterized in a transmission electron microscope (TEM, JEOL 2010, Japan) with an accelerating voltage of 200 kV. For the Cu sample subjected to tensile deformation, a 2 mm × 2 mm TEM specimen was cut from the area close to the fracture surface. Because the thickness of the tensile sample is only about 20 μm, the small square TEM sample was sandwiched in a Cu ring directly, and then twin-jet polished with an electrolyte consisting of 25% alcohol, 25% phosphorus acid and 50% de-ionized water (by volume) that was cooled in a dry ice bath.

In order to investigate the microstructure after the nanoindentation test, a rectangular Cu foil, about 3 mm × 4 mm in size, was first cut from the as-deposited sample, mechanically ground and polished on the substrate side to obtain a suitable surface finish for nanoindentation. Next, the specimen was transferred to the nanoindenter and a series of indents constituting 20 by 20 uniformly-spaced matrix was introduced in the center of the foil at a loading rate of 100 mN/s. The distance between two adjacent indents was 70 μm. The indented specimen was then punched into a 3-mm disk and glued in the center of a special glass disk at room temperature with its non-indented side up. After curing, the specimen was placed on a dimpler stage (model number D500i, South Bay Technology, San Clemente, CA) and dimpled to about 20 μm. The glue was then removed by immersing the specimen in acetone. The specimen was ion-thinned from the dimpled side by means of single-gun milling with the aid of liquid nitrogen cooling. The operating voltage was 5 kV and the tilt angle was about 10°. Finally, in order to remove possible contamination on the specimen surface, a cleaning process was performed under a voltage of 2 kV with double-gun milling for 10 min. Compared with the indenter process, deformation induced by the TEM sample preparation was negligible. The electron-transparent areas adjacent to an indent were examined in a JEOL 3010 TEM operating at 300 kV while imaging with a Gatan 622 intensified TV camera.

3. Results

3.1. Nanoindentation results

Nanoindentation experiments were conducted on each of the three materials of the same grain size: the higher twin density UFC Cu with an average twin width of 20 nm, the lower density UFC Cu with an average twin width of 90 nm, and the control UFC Cu with little

twin concentration. Further details of the microstructure are provided in the following sections.

The indentation results are shown in Fig. 1(a)–(c) for the three specimens, each of which was subjected to depth-sensing indentation at four different loading rates spanning three orders of magnitude. The loads imposed to penetrate the indenter tip into the specimen to a depth of 3 μm were higher for the specimen with the higher density of TBs. Furthermore, with increasing loading rate, a higher indentation load was required in order to impose the same displacement. A significant loading rate effect can thus be seen between the Cu samples with twin structures, over and above the normal experimental scatter associated with these experiments. However, the control UFC Cu specimen did not show any significant sensitivity to loading rate (Fig. 1(c)), beyond the normal experimental scatter. In this case, the scatter in indentation data is considerably larger than that in the other samples, which makes it impossible to clearly identify a loading rate effect on the indentation response. A similar scatter level was also observed by Schwaiger et al. [11] in their nanoindentation studies of electrodeposited UFC Ni. Although the results plotted in Fig. 1 for the twinned and control UFC specimens are restricted to loading rate control in the range of 0.1–100 mN/s, essentially the same trends have been observed for displacement rate control and strain rate control nanoindentation experiments. These results are similar to those described for untwinned NC Ni [11], where refinement of grain size from MC (microcrystalline) and UFC to NC was found to promote marked sensitivity to loading rates. Fig. 1(d) shows the load versus displacement (*P–h*) curves for the Cu specimens with different twin densities at a fixed loading rate of 0.1 mN/s. The load applied to the sample with a higher twin density is considerably larger than the load applied to the sample with lower twin density and to the UFC control Cu without twins.

The hardness of the three materials investigated in this work is plotted as a function of loading rate in Fig. 2 based on results obtained at the maximum depth of about 2800 nm. The elastic modulus of all three samples was roughly the same, and comparable to the literature value for polycrystalline Cu (~120 GPa). The

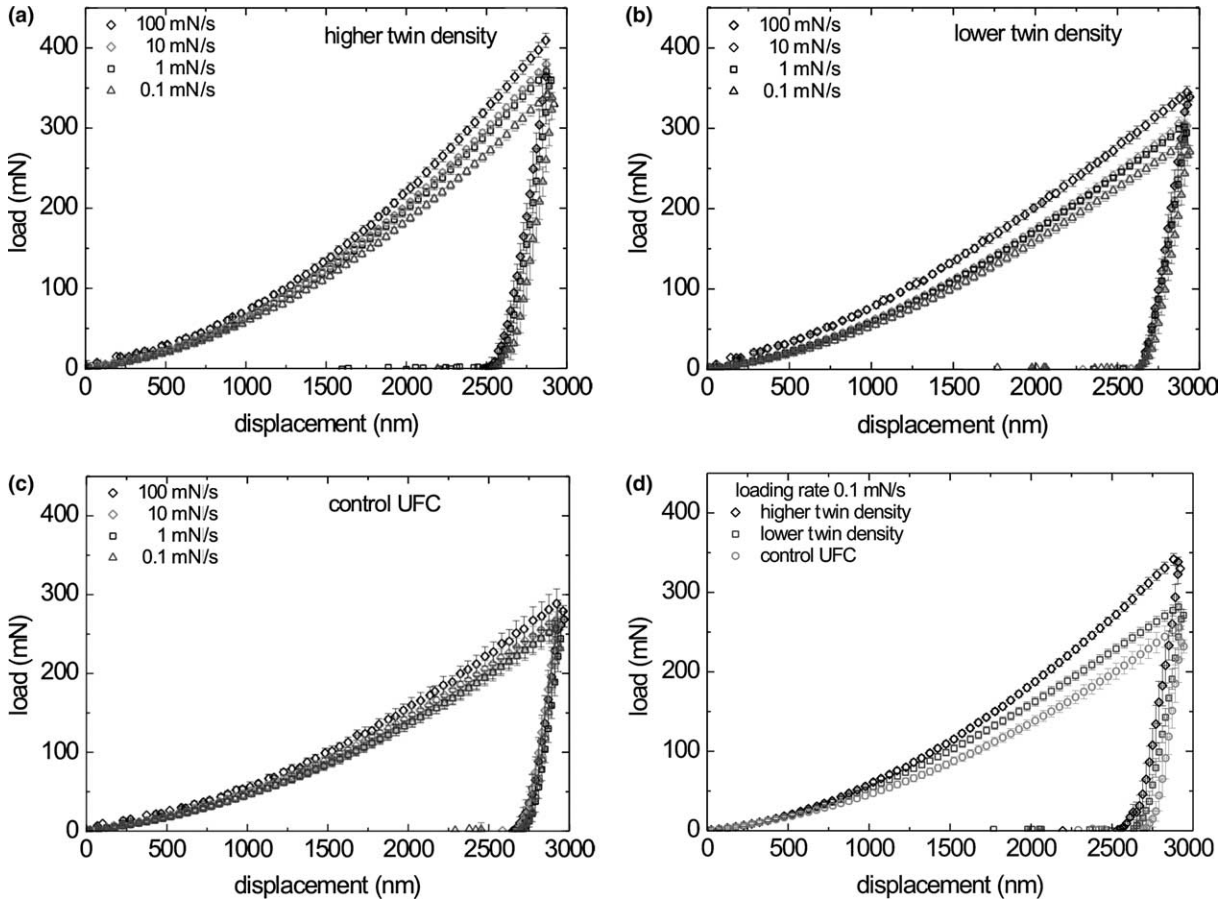

Fig. 1. Load–displacement (*P–h*) curves from nanoindentation experiments performed at four different loading rates for (a) UFC Cu with higher twin density, (b) UFC Cu with lower twin density, and (c) control UFC Cu. (d) *P–h* curves from nanoindentation experiments on the three materials at a fixed loading rate of 0.1 mN/s.

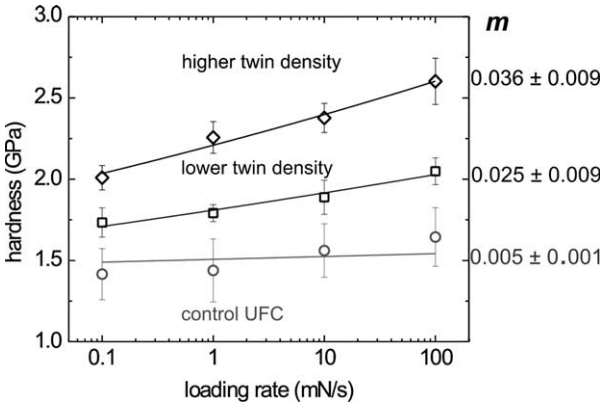

Fig. 2. Hardness from nanoindentation experiments plotted as a function of loading rate for the UFC Cu with different twin densities. The rate sensitivity exponent m was determined using the relation $\sigma \propto \dot{\varepsilon}^m$ (with the stress σ and the strain rate $\dot{\varepsilon}$) under the assumption that indentation hardness and loading rate are equivalent to stress and strain rate, respectively. Due to the large scatter in the indentation data, the rate sensitivity exponent m of the control UFC sample is obtained from σ_y in the tension tests shown in Fig. 3(c). See text for further details.

average hardness of Cu with a higher density of CTBs (2.0–2.6 GPa) is noticeably higher than Cu with a lower CTB density (1.7–2.0 GPa) or the control UFC Cu (1.4–1.6 GPa) and even higher than the hardness reported in the literature for polycrystalline pure Cu (without significant twinning) with ultra-fine sized grains [23] and nanometer sized grains [5]. For example, the typical tensile yield strength (approximated as 1/3 of hardness) of UFC Cu (with average grain size <300 nm) is less than 500 MPa [23], which is also close to the hardness measured in the UFC Cu in the present study. At a loading rate of 100 mN/s, the indentation hardness (2.6 GPa) of the Cu sample with a higher twin density is about 60% higher than that (1.6 GPa) of the UFC Cu without twins. These results indicate significant strengthening in Cu due to the higher twin density.

The loading rate sensitivity of the Cu samples, quantified through the parameter m, which is defined in Eq. (1), also depends noticeably on the twin density. For Cu with a lower twin density (average twin lamella thickness ~90 nm), $m \approx 0.025 \pm 0.009$, whereas for Cu with a higher twin density (twin lamella thickness ~20 nm) $m \approx 0.036 \pm 0.009$ within the loading rate range of 0.1–100 mN/s. For the UFC Cu without twins, due to the large scatter in the indentation response (see Fig. 1(c)), it is difficult to obtain a reliable m value from the present indentation results, so the rate sensitivity exponent m of UFC Cu without twins is instead evaluated from the tension tests (see Fig. 3(c)) where $m \approx 0.005 \pm 0.001$ within the strain rate range of 6×10^{-4} to $6 \times 10^{-1}\,s^{-1}$. The corresponding line in Fig. 2 shows that the slope of $m = 0.005$ is well within the experimental scatter.

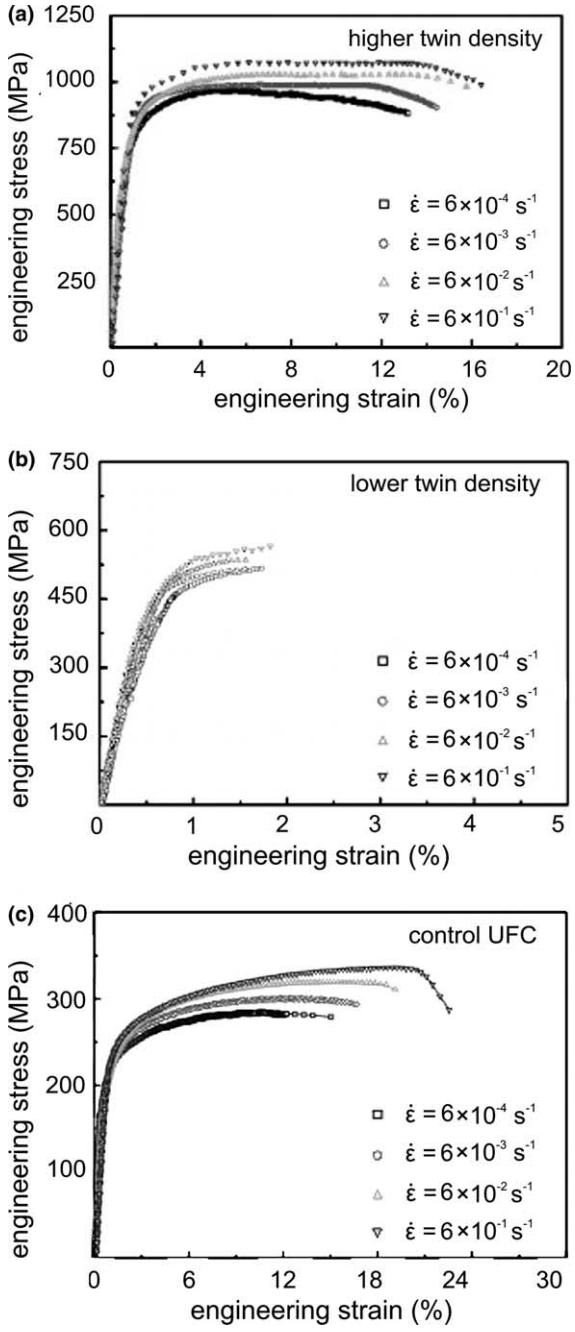

Fig. 3. Stress–strain curves from uniaxial tension at different loading rates for UFC Cu with (a) higher, (b) lower density of nano-scale twins and (c) UFC Cu (control).

The trends associated with the increased rate-sensitivity of UFC copper with nano-scale twins is also evident from tension tests conducted on the same materials. Fig. 3(a)–(c) show the tensile stress–strain curves for the UFC Cu with higher and lower twin densities as well as the UFC Cu without twins over a range of strain rates comparable to those achieved in the nanoindentation experiments (where a predominantly compressive stress state is introduced in the specimen during loading). It

is seen that Cu with a higher concentration of nanotwins also exhibits relatively higher rate-sensitivity in tension.

3.2. Microstructures of as-synthesized and deformed specimens

The as-synthesized microstructures of the higher twin density UFC Cu, the lower twin density UFC Cu, and the control UFC Cu specimens investigated in this work are shown in Fig. 4(a)–(c), respectively. These TEM images show that the Cu samples consist of roughly-equiaxed grains (Fig. 4(a) and (b)) with each grain containing a large number of growth twins (as indicated by the selected area diffraction pattern included as an inset in Fig. 4(a)) with thickness of up to tens of nm. For all of the samples with same density and purity, the average grain size is almost the same, being about 400–500 nm. However, the twin density is very different. The measurement was performed with the grain orientation adjusted to a $\langle 1\,1\,0\rangle$ zone axis. In this orientation, $(\bar{1}\,1\,1)$ and $(1\,\bar{1}\,1)$ twins are edge-on while $(1\,1\,1)$ and $(1\,1\,\bar{1})$ twins are inclined to the surface. Measurements of the lamella thickness along [1 1 0] beam direction showed the average twin thickness is about 20 nm for higher twin density UFC Cu (Fig. 4(a)) and about 90 nm for lower twin density UFC Cu (Fig. 4(b)). Only few twins could be detected in the control UFC Cu (Fig. 4(c)). The twins separate grains into nm-thick twin/matrix lamellar structures. For the as-deposited state, the vast majority of the twin boundaries are coherent and only a few trapped lattice dislocations can be seen in the larger twin lamellae.

In order to explore the mechanistic origin of the high hardness and high loading rate sensitivity in the Cu samples, the microstructures of the deformed samples were investigated in the TEM after both nanoindentation and uniaxial tension. The microstructure in the vicinity of an indentation in UFC Cu with higher twin density is shown in Fig. 5. It is evident that the indentation process induces high strains in the Cu sample; TBs are displaced due to high local strains. A high density of dislocations is visible inside the twins and at the TBs. A comparison of TEM images before (Fig. 4(a)) and after (Fig. 5) indentation reveals that the twin width is altered by severe plastic deformation. As reviewed in Christian and Mahajan [15], twin width could be affected as a result of the interaction of slip bands with twins.

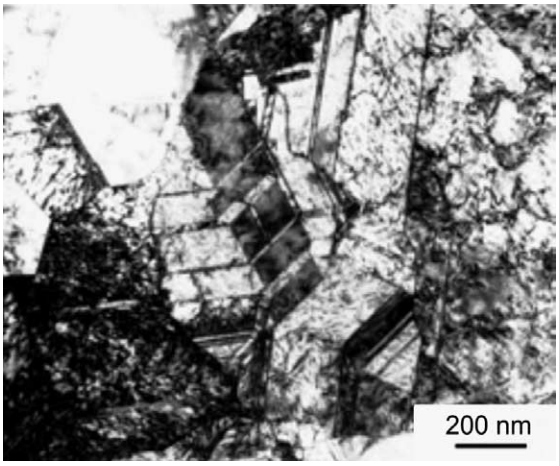

Fig. 5. TEM image of an indented Cu sample with high twin density.

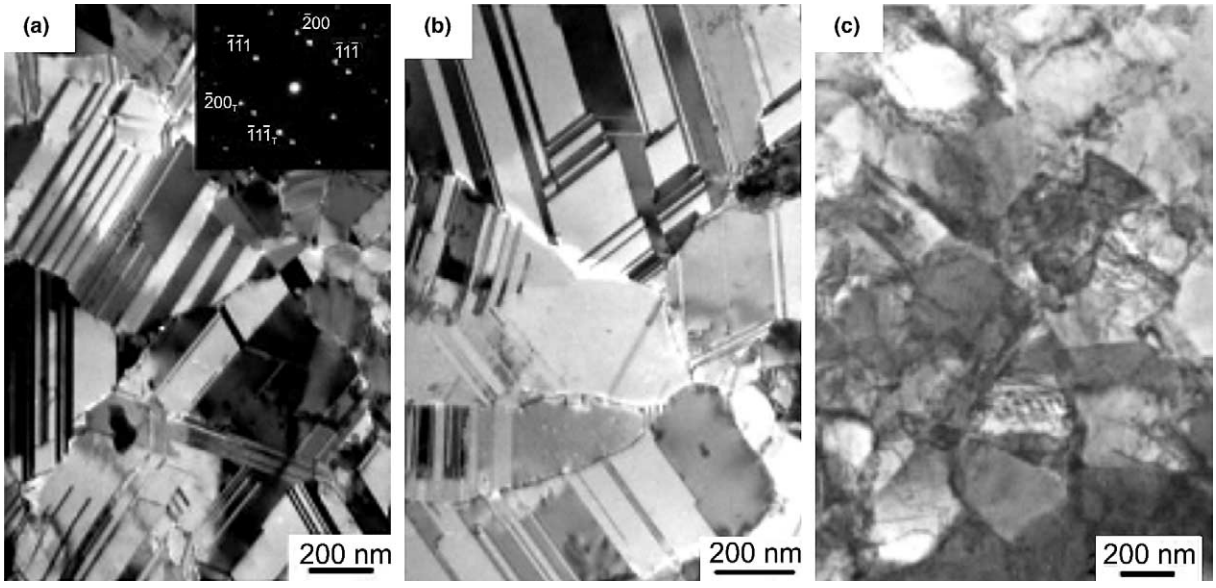

Fig. 4. TEM images of the as-processed microstructure of (a) Cu with a higher twin density, (b) Cu with a lower twin density, and (c) control UFC Cu essentially without twins.

Fig. 6 shows post-indentation TEM images of Cu with higher twin density. This image reveals a large population of dislocation debris in the vicinity of CTBs. It is clear that most CTBs in the deformed sample undergo significant displacement. Many CTBs in the deformed specimen are not straight as in the case of the undeformed sample (see Fig. 4(a)). There is evidence pointing to the displacement of CTBs; In the lower part of Fig. 6(a), the CTBs marked as "A", "B", "C" and "D" are almost parallel to one another. However, in the upper part of the same figure marked by the white square 1, the CTB marked "A" appears to be displaced more to the left whereas CTB "B" has been displaced more to the right; CTBs "C" and "D", which are close to each other, seem to be connected. The white square marked "2" in Fig. 6(a) also shows similar trends. Some CTBs seem to have "disappeared" completely on one side during the deformation process, as shown in Fig. 6(b). Note the step created in the twin boundary in the bottom center of Fig. 6(b).

Further evidence for the formation of steps in displaced CTBs in nanoindented Cu with high twin density is provided in Fig. 7. Although it is possible that growth twins can contain steps in the as-deposited condition, our extensive TEM observations did not reveal evidence for such step formation in the present sample in the as-processed state. The semicircular strain contrast at the CTB (indicated by the upward-pointing arrow) suggests possible dislocation emission from the CTB, especially near the step in the boundary. Migration of TBs and shrinkage of twins as well as of grains after deformation has recently been reported for Cu having micron-sized grains [24]. However, in our experiments no significant changes in the grain size have been found.

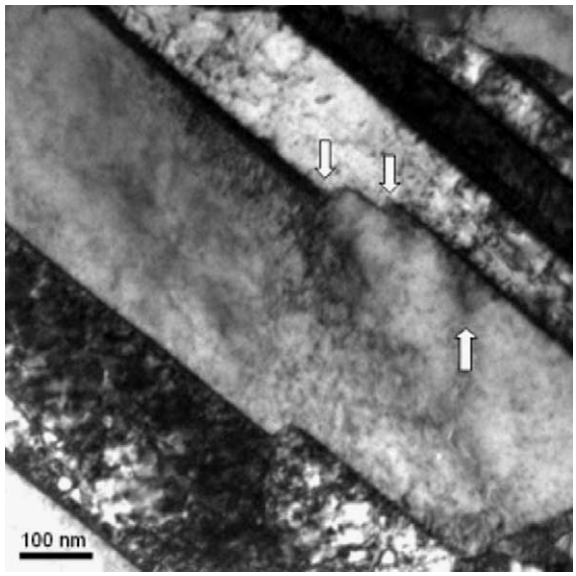

Fig. 7. Displacement of CTBs resulting in steps and jogs in the boundary, as shown by the downward pointing arrows in this post-indentation TEM image of UFC Cu with high twin density. The upward pointing arrow shows a dislocation loop apparently emitted from the twin boundary in the vicinity of the step.

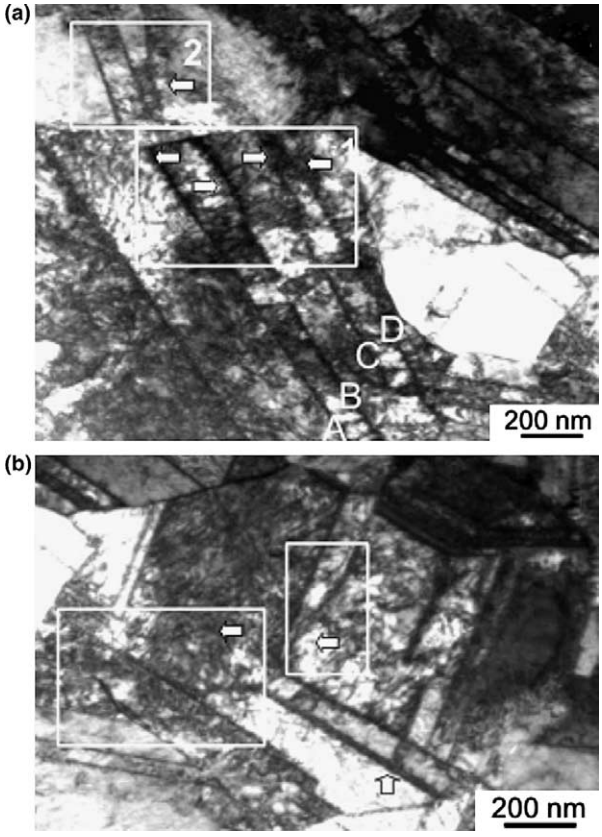

Fig. 6. Post-indentation TEM images of dislocation sources from displaced CTBs in Cu sample with higher twin density. See text for further details.

In addition to post-indentation TEM, we have performed transmission electron microscopy of UFC Cu with nano-twins after the specimen was subjected to more uniform deformation, i.e., deformation to a uniaxial tensile strain of 13%. Fig. 8 shows the microstructure of Cu with higher twin density. Numerous dislocations are present in the thick twin lamellae, whereas relatively few dislocations can be found in the thinner ones. Copious dislocation debris can also be seen in the vicinity of CTBs with spacings of several nanometers, as shown in Fig. 8(b). In order to determine the Burgers vector of the trapped dislocation, the local Burgers circuit method was employed. Crystallographic analysis using the Thompson tetrahedral shows that the closure failure is consistent with a partial dislocation with Burgers vector of $1/6\langle 1\,1\,2\rangle$ type.

The micrographs in Fig. 8 also show that in the deformed Cu sample, most CTBs are not straight as it is the case in the undeformed sample; obvious ledges are formed by the Shockley partial, as shown by the white arrow in Fig. 8(a). These microstructural changes in

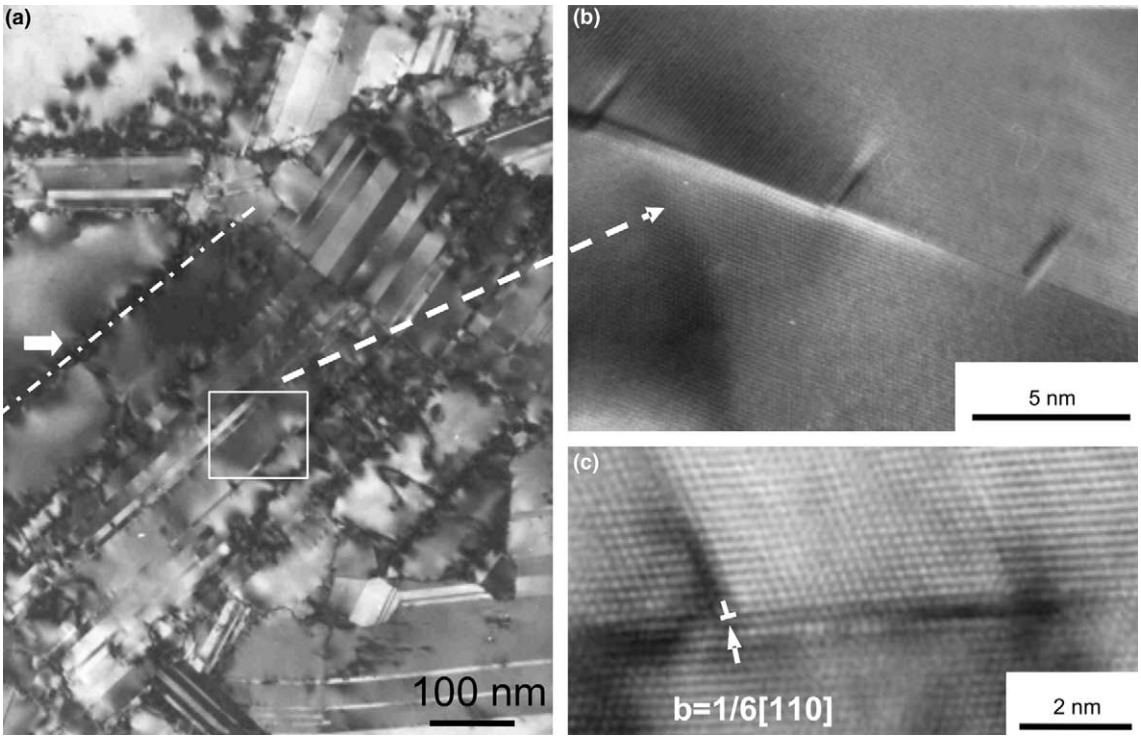

Fig. 8. TEM images of the microstructure close to the failure surface of UFC Cu with higher twin density after a tensile test.

UFC Cu with higher twin density after tensile deformation are similar to those seen after nanoindentation. In contrast to the same UFC Cu after indentation, we did not observe a clear difference of twin width after tensile testing.

Microstructure investigation of the Cu samples after deformation confirmed that the interactions between the dislocations and CTBs play a dominant role in the plastic deformation process. In general, the most probable sites for dislocation generation should be GBs and triple junctions at the initial deformation stage [25]. Once the dislocations are generated, they move through the grain interior and in most cases are blocked at twin boundaries. The blocked dislocations could pile-up but also propagate across the twins if they were to undergo dislocation dissociation reactions, which would require a stress concentration at the twin/slip band intersection. Following such interactions between slip bands and CTB, dislocation debris, such as the Shockley partials, would be left behind at the TBs. This is indeed observed in Fig. 8(c).

4. Discussion

The overall rate-dependence of a material is influenced by contributions from dislocations, grain boundary diffusion and lattice diffusion [25–28]. The contributions of lattice diffusion can in general be neglected because they are much smaller than those due to dislocation glide and boundary diffusion.

An analysis of the parameters that influence thermal activation could shed light on rate controlling mechanisms in the plastic deformation of engineering metals and alloys [26–28]. Using the definitions of strain rate sensitivity and activation volume from Eqs. (1) and (2), respectively, we derive an activation volume (v^*) of about $12b^3$ for Cu with higher twin density, and about $22b^3$ for Cu with lower twin density from the present nanoindentation experiments. These values are much smaller than v^* of the present control UFC Cu ($\sim 135b^3$). Values of m and v^* for UFC Cu with controlled nano-twin content from the present study are summarized in Table 1. Also listed in Table 1 are available values of m and v^* from the published literature [10–12,29–35] for NC, UFC and MC Cu and Ni (without a controlled population of nano-twins).

For conventional fcc metals, such as Cu, m is about 0.004 and only a weak grain size dependence of m has been found for the dislocation mechanism [33]. The activation volume of dislocation processes is usually about $800–1000b^3$. With decreasing grain size the dislocation glide mechanism is suppressed and GB diffusion gradually increases. Recently, it was shown that for fcc metals with a grain size in the sub-micrometer regime, m was high and v^* was small. For example, for ECAP and cold-rolled Cu with an average grain size of 200 nm, $m = 0.02$ and $v^* = 48b^3$ [12].

Table 1
Summary of results on the rate sensitivity of deformation of UFC copper with nano-scale twins from the present experiments, and comparisons with literature data for Cu and Ni of different grain sizes covering the NC, UFC and MC range

Material	Grain size (twin width)	m	v^*	Reference (test method used)
UFC Cu (essentially no twins)	500 nm	0.005 ± 0.001	$\sim 135b^3$	This study (tensile test)
UFC Cu (lower twin density)	500 nm (~90 nm)	0.025 ± 0.009	$\sim 22b^3$	This study (nanoindentation)
UFC Cu (higher twin density)	500 nm (~20 nm)	0.036 ± 0.009	$\sim 12b^3$	This study (nanoindentation)
MC Cu	12–90 μm	0.007–0.004	$\sim 1000b^3$	[29] (tensile test)
MC Cu	40 μm	0.006	$\sim 1000b^3$	[30,31] (tensile test)
Cold-deformed UFC Cu	200 nm	0.015	$\sim 48b^3$	[12] (tensile test)
ECAP + cold-rolled UFC Cu	300 nm	0.04	$\sim 48b^3$	[12] (compression test)
ECAP + cold-rolled UFC Cu	300 nm	0.019	$\sim 48b^3$	[12] (tensile strain rate jump test)
MC Ni	>5 μm	<~0.004		[32,33] (tensile test)
Electrodeposited NC Ni	30 nm	~0.016	$10–20b^3$	[34] (tensile test)
Electrodeposited NC-UFC Ni	20–200 nm	~0.01–0.03		[10,11] (uniaxial tension, nanoindentation)
ECAP UFC Ni	300 nm	0.006		[35] (tensile test)

Also indicated are the inferred values of activation volume where available.

Data for Ni with an average grain size of 30 nm showed strain rate sensitivity at room temperature four times as high as that of coarse-grained Ni and an activation volume of $10–20b^3$ [34]. The higher strain rate sensitivity as well as the lower v^* in NC materials indicate a different rate-limiting deformation mechanism that dominates plastic deformation. First, compared to their coarse-grained counterparts, NC materials have a significantly higher percentage of GBs and an enhanced GB diffusion. It was suggested that GB diffusion could be one of the dominant deformation mechanisms when the grain size decreases down to the nm range, especially for the grains smaller than 20 nm [4,36,37]. This was also indicated by molecular dynamics simulations, in which the GB assisted thermal activation through atomic shuffling and partial dislocation emission in the NC materials could occur [38]. Second, the interaction between dislocations and the abundant GB networks is increased and might contribute to the extraordinary rate-sensitivity of NC metals; Dislocations concentrated locally at GBs may also lead to a smaller activation volume [13]. Therefore, the rate-controlling deformation mechanism for the highly elevated values of m for fcc metals with nano-sized grains could arise from the synergistic performance of abundant GB diffusion and the interaction between dislocations and GBs.

For the present UFC Cu with nano-twins, grain boundary diffusion is not likely to be the dominant mechanism due to the large grain size. Furthermore, the contribution of dislocation sources at GBs as well as dislocation interaction with GBs appears to be very limited since m is only 0.005, as observed for UFC Cu.

In addition, dislocation glide is inhibited by the high density of CTBs. The suppression of dislocation glide is also supported indirectly by the absence of strain hardening phenomena, as found in the tensile test data for Cu with the higher twin density [18]. Therefore, the increased values of m and the strongly lowered values for v^* suggest another new rate-controlling deformation mechanism different from that known for fcc coarse-grained and UFC metals without twins. These additional contributions could arise from the large number of CTBs in the microstructure.

From the deformed microstructures obtained from our TEM studies (Figs. 6–8), three main observations can be made: (i) CTBs serve as barriers to dislocation motion; (ii) the dislocation density increases substantially with increasing twin density; and (iii) the displacement of CTBs, the formation of steps and jogs in the TBs and the apparent nucleation of dislocation loops from the boundaries, especially in the vicinity of steps, contribute to deformation.

The energy of the perfect Σ3 CTB is about 24 mJ/m^2, which is much smaller than that of a conventional GB (>600 mJ/m^2) [39]. However, CTBs with a high density of dislocations or displaced CTBs are expected to increase the boundary energy significantly. Furthermore, CTBs with a high density of defects, steps and jogs could act as dislocation sources like conventional GBs. It has indeed been found from computational simulations that defects at the CTBs assist dislocation generation [40]. Dislocations were generated from a loop joined with a step in CTBs [40]. Hence, CTBs with a density of defects or displaced CTBs do not only behave as obstacles to dislocation motion, but also serve as dislocation sources during further deformation, consistent with the present TEM observations of deformed UFC Cu with nano-twins.

The stress concentration acting upon the lead dislocation is proportional to the number of piled-up dislocations and the applied external shear stress. With decreasing twin lamella thickness, fewer dislocations are expected to pile up inside the twins. In other words, higher external stress is necessary for the dislocations to cross the CTB. If the twin lamellae are too

thin for a dislocation pile-up, a single dislocation may penetrate the CTB. In such a scenario, an extremely high stress is required for such a dislocation–CTB interaction. Rao and Hazzledine [41] estimated from MD simulation that the applied stress could be as high as 0.03μ to 0.04μ (with μ being the shear modulus), i.e., the stress could be 1.4–1.9 GPa in Cu. Therefore, the interaction of dislocations and CTBs may provide one of the principal mechanistic reasons for the high strength of twinned Cu. This supports our experimental finding of improved strength/hardness in the Cu specimen with a thinner twin lamella (i.e., higher twin density).

Our post-deformation TEM image shown in Fig. 7 indicates that TBs may also serve as sites of dislocation loops. Molecular dynamics simulations [42] have been reported that include considerations of both unstable and stable stacking fault energy in conjunction with GB defect nucleation similar to dislocation emission at the crack tip under mode I [43,44] and mixed-mode loading conditions [45,46]. Such analyses imply phenomenological responses for strain rate sensitivity that are different for different fcc metals and also point to elevated flow stress values [42,47]. Such an argument could potentially point to differences in the manner in which full or partial dislocation emission leads to rate-sensitivity and in which changes occur in the activation volume. In this context, we note recent analyses [48] in which stress concentrators such as GB facets or TBs with jogs are assumed to exist, which slip locally in a mode II or mode III crack-like manner thereby initiating partial dislocations and loops from the tip of the stress concentration. Such a dislocation model [48] leads to the rather significant result that the activation volume $v^* \sim \pi b^3$. The small values for activation volume, clearly demonstrated in the present study for the case of UFC Cu with nano-twins, provide a compelling rationale for what appears to be strong strain-rate sensitivity. This could also suggest the possibility that although the grain size is in the UFC range, the presence of higher concentration of nano-scale twins leads to greater TB migration. TEM observations of CTB displacement and jog formation in CTBs (e.g., Figs. 6 and 7) appear to support this interpretation.

5. Conclusions

(1) The loading rate sensitivity of UFC Cu with a high density of coherent twin boundaries is shown to be significantly (up to about seven times) higher than that of UFC Cu without twins. With a decrease of CTB density, the hardness and the rate sensitivity also decrease. CTBs are thus shown to play an important role in plastic deformation. The high hardness of UFC Cu with nano-scale twins originates from the effective blockage of dislocation motion by numerous CTBs.

(2) Post-deformation TEM observations in UFC Cu with higher concentration of nano-scale twins indicate noticeable displacement and movement of CTBs, formation of steps and jogs along CTBs, and the generation of high dislocation density around CTBs, especially in the vicinity of stress concentrations. These processes appear to lead to a thermal activation volume during plastic flow which is some three orders of magnitude smaller than that found for microcrystalline fcc metals.

(3) The CTBs with a high density of defects and displaced CTBs also appear to serve as dislocation sources, very much like conventional GBs.

Acknowledgements

This work was supported by the Defense University Research Initiative on Nano Technology (DURINT) on "Damage- and Failure-Resistant Nanostructured and Interfacial Materials" which is funded at MIT by the Office of Naval Research under Grant N00014-01-1-0808. The authors acknowledge use of the Nano-Mechanical Technology Laboratory at MIT and the Electron Microscopes at the National Center for Electron Microscopy at the University of California, Berkeley. L.L. and K.L. acknowledge financial support from the National Science Foundation of China (Grants 50021101 and 50201017). The authors are grateful to Prof. S. Mao for his assistance during the course of the TEM work, and they also thank Profs. S. Kumar, R.J. Asaro and Dr. Z.H. Jin for helpful discussion.

References

[1] Hall EO. The deformation and ageing of mid steel: III Discussion of results. Proc Phys Soc Lond B 1951;64:747–53.
[2] Petch NJ. The cleavage of polycrystals. J Iron Steel Inst 1953;174:25–8.
[3] Gleiter H. Nanocrystalline materials. Prog Mater Sci 1989;33(4):223–315.
[4] Kumar KS, Van Swygenhoven H, Suresh S. Mechanical behavior of nanocrystalline metals and alloys. Acta Mater 2003;51(19):5743–74.
[5] Sanders PG, Eastman JA, Weertman JR. Elastic and tensile behavior of nanocrystalline copper and palladium. Acta Mater 1997;45(10):4019–25.
[6] Gleiter H. Nanostructured materials: basic concepts and microstructure. Acta Mater 2000;48(1):1–29.
[7] Siegel RW, Fougere GE. Mechanical properties of nanophase metals. Nanostruct Mater 1995;6(1–4):205–16.
[8] Lu L, Li SX, Lu K. An abnormal strain rate effect on tensile behavior in nanocrystalline copper. Scripta Mater 2001;45(10):1163–9.

[9] Wang YM, Ma E. Temperature and strain rate effects on the strength and ductility of nanostructured copper. Appl Phys Lett 2003;83(15):3165–7.
[10] Dalla Torre F, Van Swygenhoven H, Victoria M. Nanocrystalline electrodeposited Ni: microstructure and tensile properties. Acta Mater 2002;50(15):3957–70.
[11] Schwaiger R et al. Some critical experiments on the strain-rate sensitivity of nanocrystalline nickel. Acta Mater 2003;51(17): 5159–72.
[12] Wei Q et al. Effect of nanocrystalline and ultrafine grain sizes on the strain rate sensitivity and activation volume: fcc versus bcc metals. Mater Sci Eng A 2004;381:71–9.
[13] Wang YM, Ma E. Strain hardening, strain rate sensitivity, and ductility of nanostructured metals. Mater Sci Eng A 2004;375–77:46–52.
[14] Conrad H. In: Zackey VF, editor. High strength materials.
[15] Christian JW, Mahajan S. Deformation twinning. Prog Mater Sci 1995;39(1–2):1–157.
[16] Babyak WJ, Rhines FN. The relationship between the boundary area and hardness of recrystallized catridge brass. Trans Metall Soc AIME 1960;218:21–3.
[17] Lu L et al. Ultrahigh strength and high electrical conductivity in copper. Science 2004;304(5669):422–6.
[18] Zhang X et al. Enhanced h ardening in Cu/330 stainless steel multilayers by nanoscale twinning. Acta Mater 2004;52(4): 995–1002.
[19] Zhang X et al. Nanoscale-twinning-induced strengthening in austenitic stainless steel thin films. Appl Phys Lett 2004;84(7): 1096–8.
[20] Wu BYC, Ferreira PJ, Schuh C. Nanostructured Ni–Co alloys with tailorable grain size and twin density. 2004 [submitted].
[21] Oliver WC, Pharr GM. An improved technique for determining hardness and elastic-modulus using load and displacement sensing indentation experiments. J Mater Res 1992;7(6):1564–83.
[22] Dao M et al. Computational modeling of the forward and reverse problems in instrumented sharp indentation. Acta Mater 2001;49(19):3899–918.
[23] Wang YM et al. High tensile ductility in a nanostructured metal. Nature 2002;419(6910):912–5.
[24] Field DP et al. Observation of twin boundary migration in copper during deformation. Mater Sci Eng A 2004;372(1–2):173–9.
[25] Malis T, Tangri K. Grain boundaries as dislocation sources in the premacroyield strain region. Acta Mater 1979;27:25–32.
[26] Conrad H. J Metals 1964;16:582.
[27] Cahn JW, Nabarro FRN. Thermal activation under shear. Philos Mag 2001;81(5):1409–26.
[28] Taylor G. Thermally-activated deformation of Bcc metals and alloys. Prog Mater Sci 1992;36:29–61.
[29] Follansbee PS, Kocks UF. A constitutive description of the deformation of copper based on the use of the mechanical threshold stress as an internal state variable. Acta Metall 1988;36:81–93.
[30] Carrekar RP, Hibbard WR. Tensile deformation of high-purity copper as a function of temperature, strain rate, and grain size. Acta Metall 1953;1:64–663.
[31] Follansbee PS, Regazzoni G, Kocks UF. Mechanical properties of materials at high strain rates of strain. In: Inst. Phys. Conf. Ser. 70. The Institute of Physics; 1984. p. 71.
[32] Conrad H, Narayan J. On the grain size softening in nanocrystalline materials. Scripta Mater 2000;42(11):1025–30.
[33] Conrad H. Grain size dependence of the plastic deformation kinetics in Cu. Mater Sci Eng A 2003;341(1–2):216–28.
[34] Ma E. Watching the nanograins roll. Science 2004;305(5684):623–4.
[35] Gray GT et al. Influence of strain rate & temperature on the mechanical response of ultrafine-grained Cu, Ni, and Al–4Cu–0.5Zr. Nanostruct Mater 1997;9(1–8):477–80.
[36] Schiotz J, Di Tolla FD, Jacobsen KW. Softening of nanocrystalline metals at very small grain sizes. Nature 1998;391(6667):561–3.
[37] Shan ZW et al. Grain boundary-mediated plasticity in nanocrystalline nickel. Science 2004;305(5684):654–7.
[38] VanSwygenhoven H, Derlet PM. Grain-boundary sliding in nanocrystalline fcc metals. Phys Rev B 2001;64(22):1–7.
[39] Howe JM. Interfaces in materials 1997:350.
[40] Konopka K, Mizera J, Wyrzykowski JW. The generation of dislocations from twin boundaries and its effect upon the flow stresses in fcc metals. J Mater Proc Technol 2000;99(1–3):255–9.
[41] Rao SI, Hazzledine PM. Atomistic simulations of dislocation–interface interactions in the Cu–Ni multilayer system. Philos Mag 2000;80(9):2011–40.
[42] Van Swygenhoven H, Derlet PM, Froseth AG. Stacking fault energies and slip in nanocrystalline metals. Nature Mater 2004;3(6):399–403.
[43] Rice JR. Dislocation nucleation from a Crack tip – an analysis based on the Peierls concept. J Mech Phys Solids 1992;40(2):239–71.
[44] Rice JR, Beltz GE, Sun Y. Peierls framework for dislocation nucleation from a crack tip. In: Argon AS, editor. Topics in fracture and fatigue. New York: Springer-Verlag; 1992. p. 1–58.
[45] Xu G, Argon AS, Ortiz M. Nucleation of dislocations from crack tips under mixed modes of loading: implications for brittle against ductile behaviour of crystals. Philos Mag A 1995;72(2):415–51.
[46] Xu G, Argon AS, Ortiz M. Critical configurations for dislocation nucleation from crack tips. Philos Mag A 1997;75(2):341–67.
[47] Asaro RJ, Krysl P, Kad B. Deformation mechanism transitions in nanoscale fcc metals. Philos Mag Lett 2003;83(12):733–43.
[48] Asaro RJ, Suresh S, A mechanistic model for the significantly lowered activation volume and enhanced rate sensitivity of nanograined materials. 2004 [Unpublished report].